Topographic Influences on the General Circulation of the Southern Hemisphere: A Numerical Experiment

CARLOS R. MECHOSO

Department of Atmospheric Sciences, University of California, Los Angeles, CA

(Manuscript received 7 January 1981)

ABSTRACT

A July integration of a GFDL spectral general circulation model is repeated after eliminating from the model the topographic elevations. Zonally averaged mean fields, regions of frequent cyclogenesis and cyclone tracks, and the standing waves in geopotential at 500 mb simulated for the Southern Hemisphere in both integrations are compared. It is argued that the differences in the results support the interpretation advanced by Mechoso (1980) concerning the influence of Antarctica on the general circulation of the Southern Hemisphere.

1. Introduction

One of our objectives in a recent study (Mechoso, 1980) was to assess the role of middle-latitude cyclones migrating into the Antarctic region in determining the characteristics of the atmospheric circulation around Antarctica. The problem was studied numerically with a primitive equation, three-level, hemispheric spectral model. The topography was idealized, consisting of a zonally symmetric dome centered at the pole with a meridional profile representative of East Antarctica. The model did not include any radiation, moisture or vertical diffusion schemes. It included horizontal diffusion and very basic parameterizations for surface drag and thermal interactions with the earth's surface. We performed several integrations starting from prescribed velocity and temperature distributions and analyzed the predicted time evolutions. On the basis of the results obtained in those integrations we argued that the combined action of migrating middle-latitude cyclones, the topography of Antarctica and the temperature gradients around the continent, enhances the baroclinicity of the atmosphere over the Antarctic slopes causing local cyclogenesis.

The model used in Mechoso (1980) is conceptually simple if compared to general circulation models (GCM's) with their complex parameterizations of physical processes. Perhaps one of the most conspicuous shortcomings of almost all existing GCM's is their poor performance around Antarctica, and the reasons for the presence of this feature are difficult to isolate in such a complex context. Our purpose in this paper is to expose evidence demonstrating that the mechanisms found active in the simple dynamical context of Mechoso (1980) are present and important in a GCM whose results became available when our aforementioned study was well under way. This GCM satisfies a basic prerequisite that qualifies it for this study: it performs with considerable success in the high latitudes of the Southern Hemisphere.

Manabe *et al.* (1979) present results of the integration of three spectral GFDL GCM's differing only in spectral resolution. The model with the highest resolution (rhmoboidal truncation of $M = 30$) produces, in the July experiment, a very accurate simulation of the position, intensity, and local features characterizing the low sea level pressure belt around Antarctica. We choose that model to conduct this study after considering such a skill. To put in evidence the influence of topography in determining characteristic features of the atmospheric circulation we proceeded as in Manabe and Terpstra (1974), i.e., we repeated the July experiment after eliminating from the model the topographic elevations. In what follows we describe results obtained in the case when mountains were included and their counterparts when mountains were not included, and analyze in some detail the differences in cyclogenesis and cyclone behavior in both experiments. We restrict our consideration to the extratropical latitudes of the Southern Hemisphere.

We begin in Section 2 by describing the differences between zonally averaged mean fields obtained in both integrations. In Section 3 we describe the regions of cyclogenesis and cyclone tracks obtained in both experiments and in Section 4 we study the first four zonal harmonic standing waves in geopotential at 500 mb. A brief descrip-

0027-0644/81/102131-09$06.25

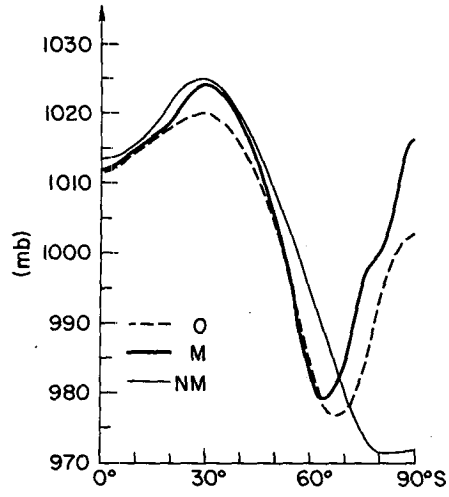

FIG. 1. Latitudinal distribution of zonally averaged mean sea level pressure.

tion of the GCM used in this study is in the Appendix and we refer the reader to Manabe *et al.* (1979) for a detailed description of the model and its performance.

2. Zonally averaged mean fields

Fig. 1 shows the latitudinal distribution of the zonally averaged mean sea level pressure obtained in the mountain (M) and no-mountain (NM) experiments, together with the observed (O) distribution. The latter was obtained from the twice-daily ANMRC (Australian Numerical Meteorology Research Center) analyses for July 1979, which include information provided by the drifting buoys deployed during FGGE. Inspection of Fig. 1 reveals that the subtropical highs around 30°S simulated in the M experiment are somewhat stronger than observed, while the low-pressure belt in high latitudes is slightly weaker and located a few degrees equatorward of the observed. The variation of sea level pressure with latitude in the region between 40 and 60°S is accurately captured, and results in a successful simulation of the middle-latitude belt of strong westerlies present in the Southern Hemisphere. The simulation over Antarctica is poor but Manabe *et al.* (1979) point out that the corresponding values might be strongly affected by the scheme used to reduce surface pressure to sea level. It is apparent that the performance of this model in extratropical latitudes of the Southern Hemisphere is considerably more successful than those of the models used in the studies performed by Manabe and Terpstra (1974) and Kasahara and Washington (1969). Fig. 1 also reveals that the distributions obtained in the M and NM experiments compare quite differently in both sides of a line of demarkation between 40 and 50°S: they are very similar equatorward of that boundary and drastically different poleward. In the latter region, the values corresponding to the NM experiment decrease toward the pole until around 80°S after which they slightly increase. Such a pattern indicates that the surface westerlies in the NM experiment are weaker and extend further poleward than in the M experiment, and that the region of surface easterlies in high latitudes is considerably reduced.

Fig. 2 shows the latitude-height distribution of the difference between the zonally averaged mean zonal velocities obtained in the two experiments. The greater extent of the shaded area indicates a general tendency towards higher velocities in the NM experiment, in which the mountain-induced drag is absent. Furthermore, there are substantial negative values, whereas the positive values are small. In particular, the jet stream in the upper troposphere of midlatitudes is more intense in the NM experiment, a result similar to that of Manabe and

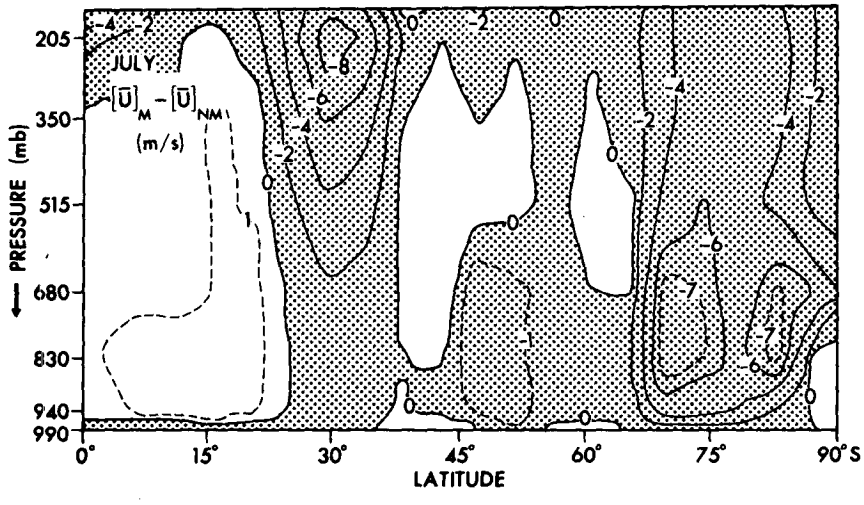

FIG. 2. Latitude-height distribution of the difference between zonally averaged mean zonal velocities simulated in the M and NM experiments.

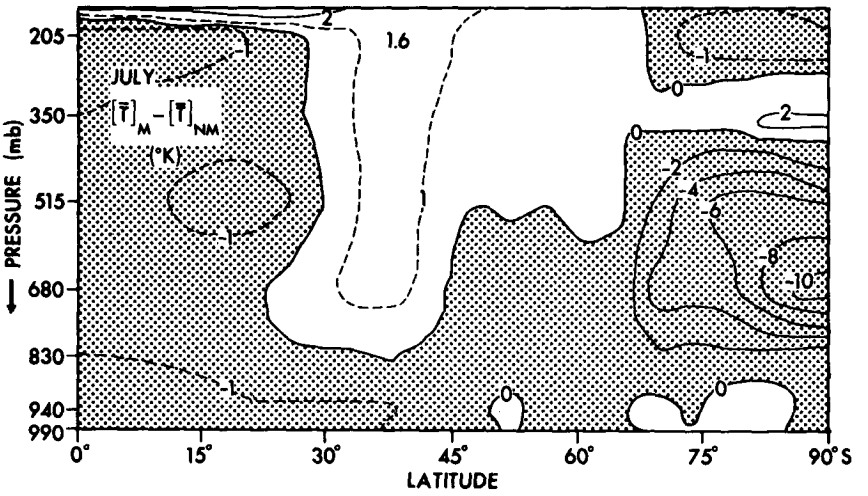

FIG. 3. As in Fig. 2 except for temperatures.

Terpstra (1974) for the Northern Hemisphere in their January simulation. Other important differences are apparent over the Antarctic region, where the values obtained in the NM experiment are higher than those in the M experiment throughout the atmosphere. The differences are pronounced in the lower troposphere, indicating a reduction of the mid-tropospheric vertical shears at latitudes corresponding to the Antarctic slopes.

Fig. 3 displays the difference between zonally averaged mean temperatures. The warming of the atmosphere over the Antarctic region in the NM experiment is remarkable, although the mean temperatures for the entire atmosphere in both experiments differ by <1 K. The warming reduces the magnitude of the meridional temperature gradients in subpolar latitudes and, consequently, the local vertical shear of the geostrophic wind. The opposite is true ~30°S where vertical shears are greater in the NM experiment.

The latitudinal distribution of zonally and vertically averaged mean northward transport of absolute angular momentum by eddies is shown in Fig. 4. The observed distribution (labeled O), was taken from Oort and Rosenstein (1981). The latitudinal variation of the momentum transport in the M experiment is in good qualitative agreement with that computed from observations, although the magnitudes are somewhat overestimated at almost all latitudes indicating that the simulated eddy activity is intense. The latitudes at which the transport reverses its sign or reaches a local maximum are accurately captured. Of particular note is that the observed equatorward transport of westerly momentum by eddies over Antarctica during July is present in the results obtained in the M experiment and absent in those obtained in the NM experiment. In the latter case, the convergence of westerly momentum is reduced between around 45°S and the Antarctic coast, while increased at subpolar latitudes resulting in a poleward extension of the middle-latitude belt of westerlies. The remarkable difference in the momentum transport between the experiments is not found in the results discussed by Manabe and Terpstra (1974). One of the findings of that study was that the contribution of the stationary eddy component to the transports of momentum and heat is relatively small in the Southern Hemisphere. Similar considerations apply to the results described in this study and consequently the values in Fig. 4 are representative of the transient eddy component.

The distribution of zonally and vertically averaged mean northward transport of heat by eddies is shown in Fig. 5. Observations indicate that to the south of around 75°S there is a region of equatorward heat transport with a stronger band of poleward heat transport to the north. Southward heat transports

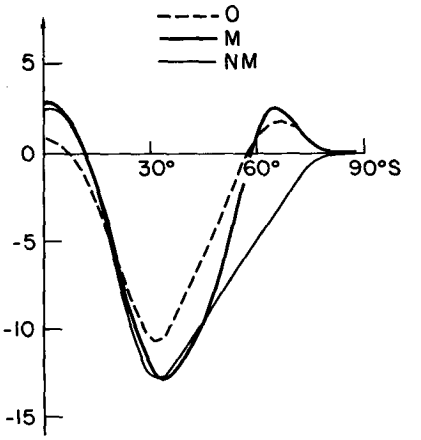

FIG. 4. Latitudinal distribution of zonally and vertically averaged mean northward transport of absolute angular momentum by eddies. Units are 10^6 m^3 s^{-2}.

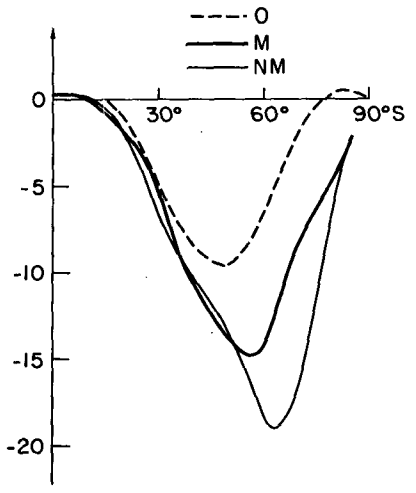

FIG. 5. As in Fig. 4 except for heat. Units are K m s^{-1}.

larger than the observed prevail at all extratropical latitudes in both simulations.

The simulated distributions disagree markedly with each other in the region south of around 50°S. In particular, the larger convergence obtained in the NM experiment confirms the expectation that in this case the eddies are largely responsible for the warming of the atmosphere over Antarctica.

3. Cyclogenesis and movement of cyclones

We recorded a sequence of evolution for a low-pressure center when a closed contour in the model generated daily maps of sea level pressure (plotted with a 4 mb contour interval) could be followed for at least two consecutive days. The first observed position of the low in such a sequence was defined as the location of cyclogenesis. The locations of cyclogenesis for July and August and the cyclone tracks for July are shown in Figs. 6 and 7 for both the M and NM experiments. A solid dot at the beginning of a track and an arrow at the end of it indicate the first and last positions respectively were detected in July.

Fig. 6 shows that in the M experiment there is frequent cyclogenesis in middle latitudes. Prominent are the high frequencies east of South America, south east of Africa, east of Australia and central Pacific. Some lows (with the characteristics of tropical cyclones) are detected over the tropical western Pacific. Few lows develop over the eastern part of the subtropical oceans. For some time after their generation, the movement of the middle-latitude cyclones is mostly in a southeast direction. The tracks become more tortuous but with a general tendency to the east near the Antarctic coast. A notable feature is that, in the M experiment, there is also high frequency of cyclogenesis at high latitudes, albeit some of the corresponding sequences of evolution are short. A perusal of the observational studies by Taljaard (1972) and Streten and Troup (1973) concerning cyclogenesis and movement of cyclones in the Southern Hemisphere reveals that the results obtained in the M experi-

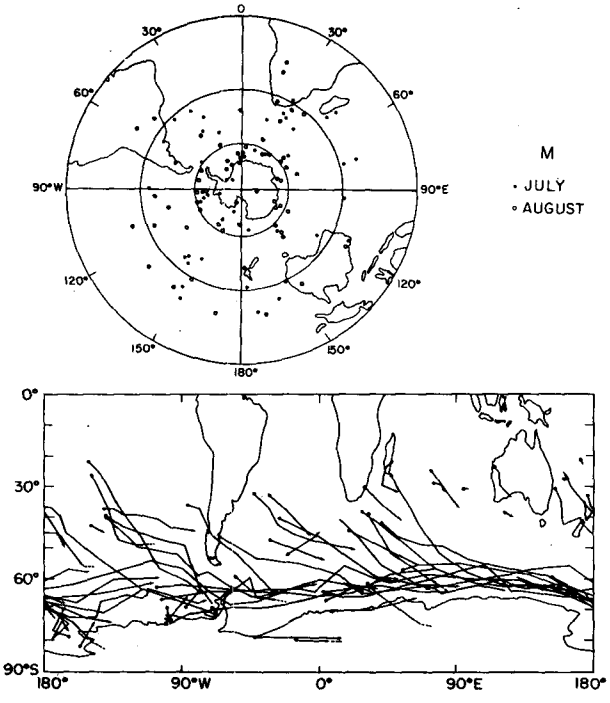

FIG. 6. Locations of cyclogenesis and cyclone tracks simulated in the M experiment.

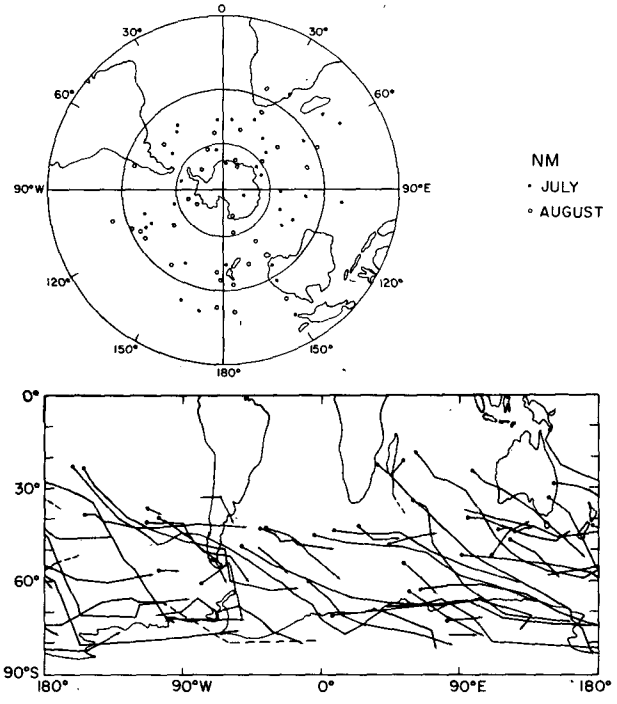

FIG. 7. As in Fig. 6 except for the NM experiment.

ment exhibit several features in agreement with available observations. Some of these features are the characteristics of the zonal variation in the frequency of cyclogenesis in middle latitudes, the poleward progression and subsequent clustering of the lows around Antarctica, the presence of a northward component in the movement of cyclones which approach the Drake Passage, and the tendency of systems not to penetrate into East Antarctica. The existence of frequent cyclogenesis in high latitudes is a controversial subject among synoptic meteorologists, as discussed by Mechoso (1980).

Fig. 7 shows that in the NM experiment the variability in the locations of cyclogenesis and in the tracks of lows is considerable. Major differences with the M case are the comparatively more irregular distribution of middle-latitude cyclogenesis, the comparatively greater tendency of the lows to move in the zonal direction after their generation, the absence of clustering of the tracks in the region around Antarctica, and the penetration of some tracks into East Antarctica. Furthermore, the simulated frequency of cyclogenesis in the NM experiment is considerably reduced. A similar scattering in the location of cyclogenesis and cyclone tracks when topographic elevations were not included in the model is apparent in the results obtained for the northern atmosphere by Manabe and Terpstra (1974), and Washington *et al.* (1977) in January simulations (the corresponding results for the Southern Hemisphere are not presented in those studies). Such a similarity indicates that the effects of the large-scale topographic features of the Southern Hemisphere, that is the Andes, the African plateau and the massive ice dome of East Antarctica, are not just confined to their vicinity (e.g., lee cyclogenesis).

4. Standing waves

Standing waves in the Southern Hemisphere have a barotropic structure (van Loon and Jenne, 1972) and their associated heat transports are small (van Loon, 1979). van Loon *et al.* (1973) proposed that such a situation is possible only over an ocean that is continuous around the earth. We expect the dynamic effects of topography to be very important in determining the standing circulation in the Southern Hemisphere. In this section we describe the standing waves in the geopotential field at 500 mb simulated in both the M and NM experiments.

Fig. 8 shows the distribution in latitude of the total zonal variance in the mean geopotential field at 500 mb obtained in the M experiment, as well as the contribution to that variance of the waves 1–4. The simulated distribution of the total variance exhibits three local maxima. The strongest maximum is reached around 60°S, there is another maximum at polar latitudes around 75°S, and the weakest maximum is reached in the subtropics around 30°S. A region where there is small variance is present between 40 and 45°S. The contribution of wave 1 to the total variance is generally dominant at all latitudes except at those with small

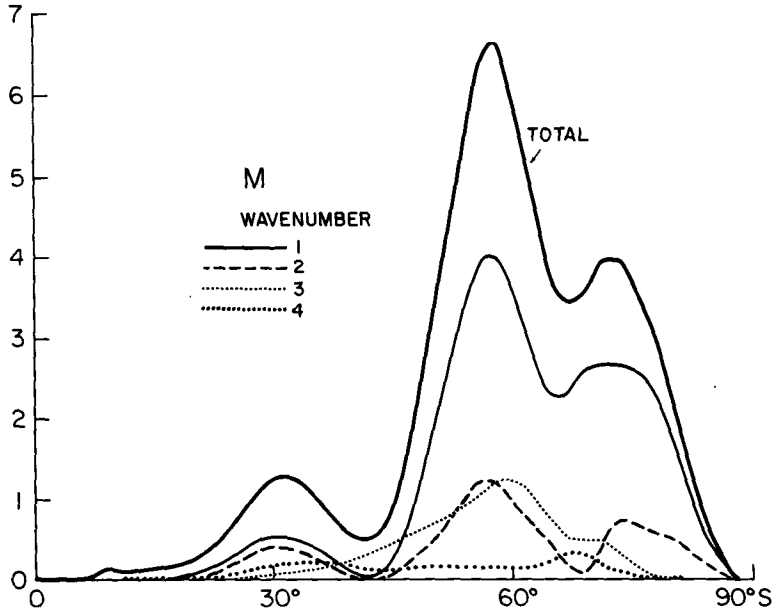

FIG. 8. Latitudinal distribution of the total zonal variance in the mean geopotential field at 500 mb simulated in the M experiment, and contributions of waves 1–4 to that variance. Units are 10^3 m^2.

variance where wave 3 becomes dominant. The standing wave 3 reaches its peak amplitude around 60°S and its contribution to the variance is small at subtropical latitudes and over Antarctica. Wave 2 has greatest amplitudes at latitudes in which the total variance reaches local maxima, in particular over Antarctica. The simulated contribution of wave 4 is generally small at all latitudes and comparatively more important in the subtropics. These results are in qualitative agreement with the observations compiled by van Loon and Jenne (1972) in that wave 1 is largest and in July has a strong peak at subpolar latitudes, two other peaks at subtropical and polar latitudes, and almost disappears near 40°S. According to Trenberth (1980) wave 2 has greatest amplitudes between 50 and 60°S and near 75°S. van Loon and Jenne (1972) point out that wave 3 reaches its peak amplitude in July at latitudes which are about 10° poleward than those obtained in the M experiment.

The distribution of the geopotential variance at 500 mb in the NM experiment is shown in Fig. 9. The total variance is greatest in two regions centered around 35 and 75°S. The subtropical maximum is stronger than that reached in the M experiment whereas the subpolar maximum is weaker. The location of the region where there is small variance is displaced about 10° poleward. The predominance of wave 1 is most notable in this case, and only wave 2 provides a sizeable (and almost constant) contribution in the region between 50 and 70°S.

The phases of the first four zonal harmonic standing waves in geopotential at 500 mb are indicated by the positions of the troughs in Fig. 10. The observed (O) positions were computed from the mean fields compiled by Oort and Rosenstein (1981). The agreement between the simulated position of the trough of wave 1 in the M experiment and that observed by Oort and Rosenstein (1981), van Loon and Jenne (1972) and Trenberth (1980), is excellent at subpolar latitudes. There is a large phase shift in the region between 40 and 45° where the variance is small and the agreement becomes poor north of this region. Note the apparent association between the locations of the trough of wave 1 and the band of high cyclone frequency from southeast of Africa to Antarctica. The most striking feature of the wave 1 in the NM experiment is the large change in phase with latitude. Thus, the geopotential field at 500 mb in the NM experiment is dominated by the contribution of one wave whose phase varies rapidly with longitude. One can tentatively conclude that such a feature is associated with the variability in the location of cyclogenesis and in the tracks of lows found in this case.

To the south of the middle-latitude region where the variance in geopotential is small, the agreement between the positions of the troughs of waves 2 and 4 with those observed is substantial, while that of wave 3 is poorer. North of that region, the agreement is generally deficient in all cases.

An important question which has not yet been addressed here concerns a possible correlation between the simulated locations of regions of preferential developments of cyclones and the long planetary waves. Frederiksen (1979) used a two-layer spherical quasi-geostrophic model to study the instability of basic flows consisting of zonal components plus

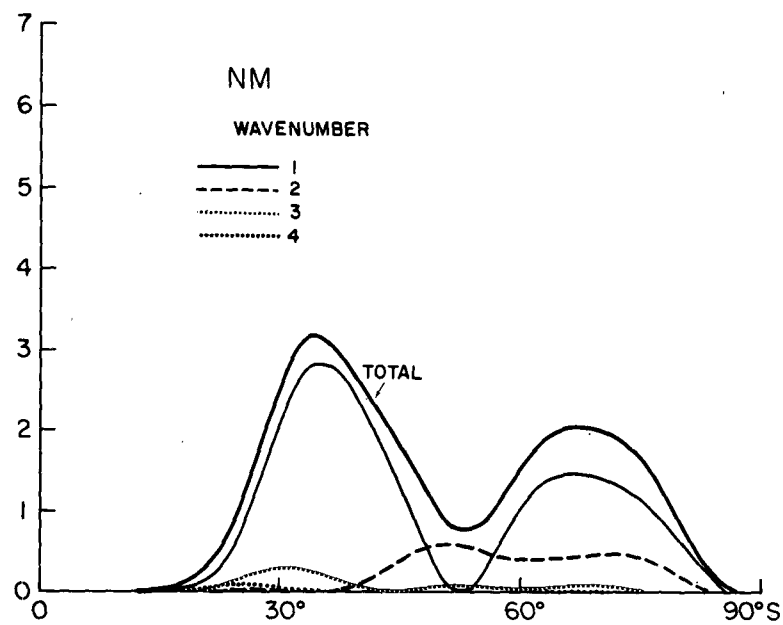

FIG. 9. As in Fig. 8 except for the NM experiment.

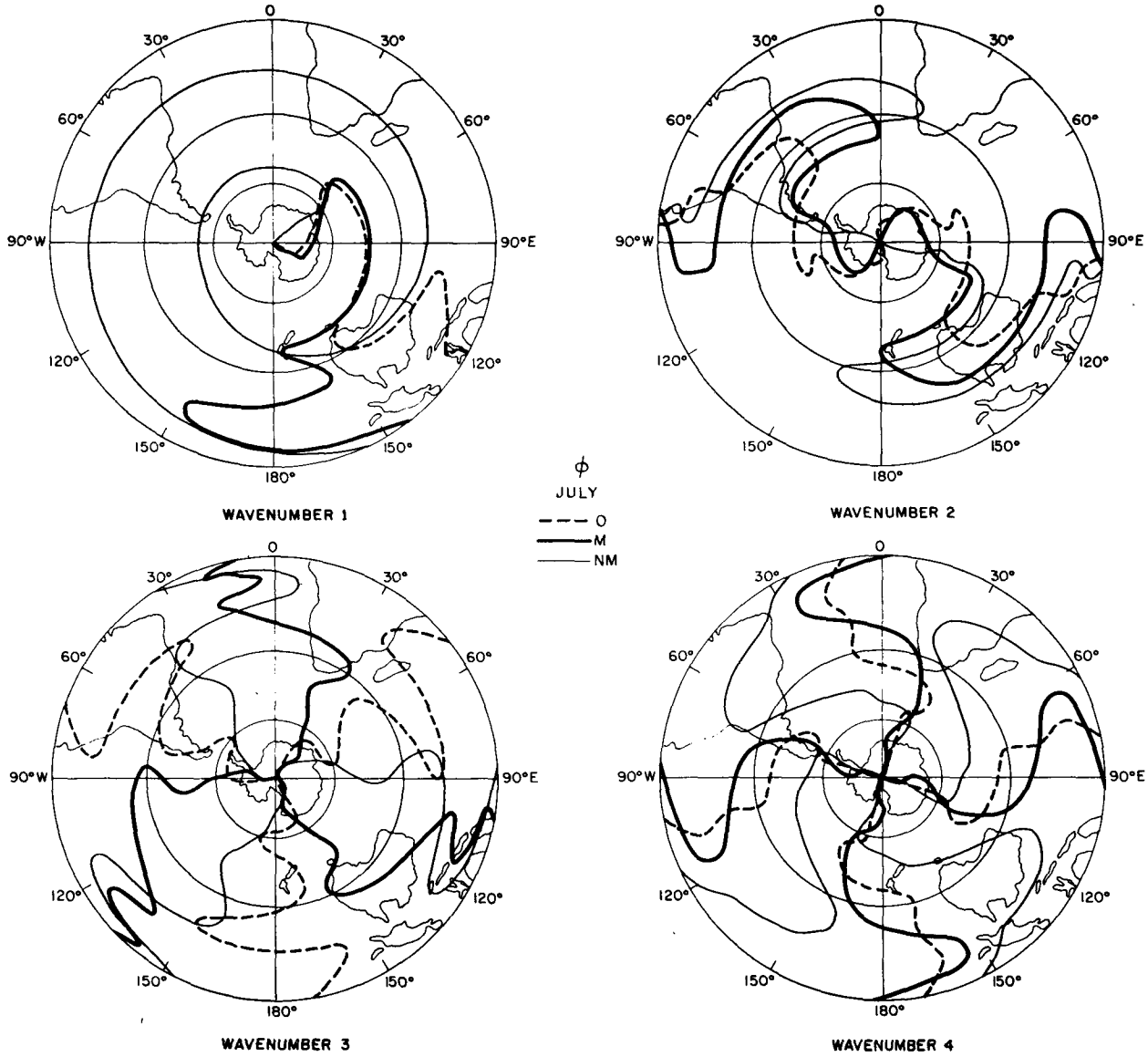

FIG. 10. Positions of troughs of the first four zonal harmonic standing waves in geopotential at 500 mb.

long waves. Niehaus (1980) analyzed the instability of flows consisting of a mean zonal component and a tilted, forced, standing wave. The results of those studies indicate that preferred regions for cyclogenesis (and anticyclogenesis) occur downstream of the positions of maximum excess shear. Frederiksen (1979) emphasizes the role of the upper layer wave in producing regions of preferential development downstream of longwave troughs. Yasunari (1977) performed harmonic analyses of the zonal distribution of average brightness along four latitudes (25°, 35°, 45°, and 55°S), and suggested patterns of relationship between regions of high brightness and the standing waves in the geopotential field. According to the proposed correlations, regions of high average brightness (considered as an indication of high frequency cloud cover, i.e., cyclone frequency) are approximately one-quarter wavelength downstream of the troughs of the standing waves. Application of this criterion to the locations of frequent cyclogenesis and standing waves simulated in the M experiment would indicate that the regions of frequent cyclogenesis in the central Pacific and south east of Africa are associated with wave 2, in agreement with Yasunari's (1977) conclusion concerning the relevance of this wave at middle latitudes. Regions of frequent development east of the major continents would be linked to wave 3, while wave 4 would be associated with the cyclogenesis around 30° east of South America and Africa, and west of Australia. Wave 4 would also contribute to the frequent cyclogenesis

in the subtropical latitudes of the central Pacific. The relevance of wave 4 at the lower middle latitudes is also in qualitative agreement with the conclusions reached by Yasunari (1977).

5. Concluding remarks

The total length of the integration of the NM experiment may not be long enough to allow us to draw conclusions of climatological character from the results. Nonetheless, the results described in the previous sections strongly suggest the following considerations of dynamical nature.

The role of the mountains appears to be fundamental to the presence of both synoptic features and features in the eddy statistics which are distinctive characteristics of the Southern Hemisphere. Among the former we include the frequency of middle-latitude cyclogenesis and the locations in the hemisphere of regions of preferential development of cyclones. Among the latter we include the magnitudes of the mean eddy transport of momentum and heat together with their associated convergences. In the NM experiment, the transport of heat by eddies to the atmosphere over Antarctica is enhanced while the convergence of westerly momentum in high latitudes is reduced. In consonance with this behavior of the eddies, the atmosphere over Antarctica is warmer and the vertical shears over the Antarctic coast are reduced. Furthermore, the simulated cyclogenesis in high latitudes around Antarctica is substantially less frequent than in the M experiment.

On the basis of these results we would argue that the mechanisms proposed by Mechoso (1980) are active in this particular GCM and support the interpretation advanced in that work concerning the influence of Antarctica in the general circulation of the Southern Hemisphere. One of the bases in that interpretation is the presence of constraint on the poleward migration of the cyclones by the elevated topography of Antarctica. If cyclones are not allowed to go poleward beyond a certain latitude, there will be a local warming that will increase the magnitude of the meridional temperature gradients poleward of this latitude. The resulting increase in the vertical shears would cause local cyclogenesis around Antarctica.

The performance in high latitudes of the GCM used in the July M and NM experiments described in this paper is not equally successful in a January integration (Manabe *et al.*, 1979). A peculiar result obtained in that integration is the strong intensity of the subpolar pressure belt in the Northern Hemisphere. We also analyzed the differences between the results obtained for the Southern Hemisphere in January M and NM experiments, but found that they are much less significant than for July. Above all, the simulated eddy activity exhibits a marked seasonal change that exceeds that observed in the Southern Hemisphere. Such a variation makes us hesitant to take the January M results as the control for a NM experiment.

While we are on the subject of the generally poor performance of almost all existing GCM's in the region around Antarctica, a few comments are in order. Those models may greatly differ in several design features, among which the numerical scheme, the schemes adopted for parameterization of subgrid-scale processes, the vertical extension of the integration domain and the grid resolution are most relevant. The choice of grid resolution represents a balance between accuracy and availability of computer resources. Manabe *et al.* (1979) found that the simulation of July mean sea level pressure with GFDL spectral models (i.e., for a given set of equations and numerical scheme) generally improves with spectral resolution. Indeed higher resolution allows a more accurate representation of topographic elevations and, consequently, the simulation of topographically forced motions is improved. Higher resolution also implies more accuracy in the simulation of the time evolution of finite amplitude baroclinic waves. Based on these considerations we may surmise that the grid resolution in several GCM's is too coarse in middle-latitudes where the vortices are generated and migrate, as well as in the region around Antarctica which is characterized by a persistent high concentration of decaying cyclones in the presence of steep topography. However, more realistic GCM's have not perforce yielded more realistic simulations of the intensity of the low-pressure belt around Antarctica as is apparent after inspection of the performance of two-level GCM's presented by Mintz (1965) and Schlesinger and Gates (1980). This feature is a manifestation of the complex interaction between the GCM numerics and physics and warrants further investigation.

Acknowledgments. Special thanks are due to Dr. S. Manabe for his valuable suggestions and for his encouragement to complete this work. We thank Mr. D. G. Hahn and Mr. L. Dimmick for his assistance with the GCM history tapes. Ms. Julia Lueken typed the manuscript and Ms. B. Gladstone assisted with the figures. This research was partially supported by the National Science Foundation, Climate Dynamics Program, under ATM 78-01922.

APPENDIX

The GCM

The GCM used in this study is one of those developed at the Geophysical Fluid Dynamics Laboratory (GFDL) by the Climate Dynamics Group.

The model has nine unevenly spaced sigma levels in the vertical (σ = pressure/surface pressure) and the variables at each sigma level are represented by truncated series of spherical harmonics. If λ is the longitude, μ (the sine of) the latitude and t the time, a model variable is written as a truncated series of spherical harmonics

$$F(\lambda, \mu, \sigma, t) = \sum_{m=-M}^{M} \sum_{n=|m|}^{|m|+M} F_n^m(\sigma, t) P_n^m(\mu) e^{im\lambda},$$

where $P_n^m(\mu)$ is an associated Legendre function. In this particular model $M = 30$. The tendency of the variables is reduced by including diffusion terms of the form $-K\nabla^2(\nabla^2 F)$, where K is a constant and ∇^2 is the two-dimensional Laplacian operator. The representation of the physical processes is nearly identical with that used in previous GFDL GCM's. The distributions of carbon dioxide and ozone are prescribed. The cloud cover is assumed to be zonally uniform and invariant with respect to time. The diurnal variation of insolation is not taken into account, and a scheme of moist convective adjustment is included. The sea surface temperatures and surface albedos over oceans and land are prescribed, these being higher whenever snow cover or sea ice are simulated. Initial conditions for both the M and NM July experiments are taken from the 31 May results obtained with a lower resolution (rhomboidal truncation of $M = 21$) spectral GCM.

REFERENCES

Frederiksen, J. S., 1979: The effects of long planetary waves on the regions of cyclogenesis: Linear theory. *J. Atmos. Sci.*, **36**, 195–204.

Kasahara, A., and W. M. Washington, 1969: Thermal and dynamical effects of orography on the general circulation of the atmosphere. *Proc. WMO/IUGG Symp. Numerical Weather Prediction*, Tokyo, Japan Meteor. Agency, IV47–IV56.

Manabe, S., and T. B. Terpstra, 1974: The effects of mountains on the general circulation of the atmosphere as identified by numerical experiments. *J. Atmos. Sci.*, **31**, 3–42.

——, D. G. Hahn and J. L. Holloway, Jr., 1979: Climate simulations with GFDL spectral models of the atmosphere: Effect of spectral truncation. *GARP Publ. Ser.*, No. 22, 41–94.

Mechoso, C. R., 1980: The atmospheric circulation around Antarctica: Linear stability and finite amplitude interactions with migrating cyclones. *J. Atmos. Sci.*, **37**, 2209–2233.

Mintz, Y., 1965: Very long-term global integration of the primitive equations of atmospheric motion. WMO Tech. Note No. 66, 141–167.

Niehaus, M. C. W., 1980: Instability of nonzonal baroclinic flows. *J. Atmos. Sci.*, **37**, 1447–1463.

Oort, A. H., and M. R. Rosenstein, 1981: Global Atmospheric Circulation Statistics, 1958–1973. NOAA Prof. Paper, U.S. Govt. Printing Office, Washington, DC. (in preparation).

Schlesinger, M. E., and W. L. Gates, 1980: The January and July performance of the OSU two-level atmospheric general circulation model. *J. Atmos. Sci.*, **37**, 1914–1943.

Streten, N. A., and A. J. Troup, 1973: A synoptic climatology of satellite observed cloud vortices over the Southern Hemisphere. *Quart. J. Roy. Meteor. Soc.*, **99**, 56–72.

Taljaard, J. J., 1972: Synoptic meteorology of the Southern Hemisphere. *Meteorology of the Southern Hemisphere*, C. W. Newton, Ed., *Meteor. Mongr.*, No. 35. Amer. Meteor. Soc., Chap. 8.

Trenberth, K. E., 1980: Planetary waves at 500 mb in the Southern Hemisphere. *Mon. Wea. Rev.*, **108**, 1378–1389.

van Loon, H., 1979: The association between latitudinal temperature gradient and eddy transport. Part I: Transport of sensible heat in winter. *Mon. Wea. Rev.*, **107**, 525–534.

——, and R. L. Jenne, 1972: The zonal harmonic standing waves in the Southern Hemisphere. *J. Geophys. Res.*, **77**, 992–1003.

——, R. L. Jenne and K. Labitzke, 1973: Zonal harmonic standing waves. *J. Geophys. Res.*, **72**, 4463–4471.

Washington, W. M., B. Otto-Bliesner and G. Williamson, 1977: January and July simulation experiments with the 2.5° latitude-longitude version of the NCAR General Circulation Model. Volume 1: Text, Volume 2: Figures. NCAR/TN-123 + STR, National Center for Atmospheric Research, Boulder [NTIS PB-270 679/4].

Yasunari, T., 1977: Stationary waves in the Southern Hemisphere midlatitudes zone revealed from average brightness charts. *J. Meteor. Soc. Japan*, **55**, 274–285.